Ageing Research Reviews 50 (2019) 1–8

Contents lists available at ScienceDirect

Ageing Research Reviews

journal homepage: www.elsevier.com/locate/arr

Review

Neuroinflammation in mild cognitive impairment and Alzheimer's disease: A meta-analysis

Steven Bradburn[a,*], Christopher Murgatroyd[a], Nicola Ray[b]

[a] Bioscience Research Centre, Manchester Metropolitan University, Manchester, United Kingdom
[b] Department of Psychology, Manchester Metropolitan University, Manchester, United Kingdom

ARTICLE INFO

Keywords:
Mild cognitive impairment
Alzheimer's disease
Neuroinflammation
Positron-emission tomography
Inflammation

ABSTRACT

Background: Increasingly, evidence from brain imaging supports the role of neuroinflammation in dementia progression. Yet, it is not clear if there are patterns of spatial and temporal susceptibility to neuroinflammatory processes in the brain that may correspond to dementia staging or symptom expression.
Methods: We searched literature databases for case-control studies examining levels of translocator protein (TSPO) levels using positron emission tomography, representing neuroinflammation, in regional analyses between healthy controls and mild cognitive impairment (MCI) or Alzheimer's disease (AD) subjects. Standardised mean differences (SMDs) were calculated and results meta-analysed using random-effects models. Quality assessments, sensitivity analysis, subgroup analysis and meta-regressions were also performed.
Results: Twenty-eight studies comprising 755 (HC = 318, MCI = 168, AD = 269) participants and 37 brain regions were included. Compared to HCs, AD participants had increased TSPO levels throughout the brain (SMD range: 0.43–1.76), especially within fronto-temporal regions. MCI subjects also had increased TSPO levels, mainly within the neocortex, with more modest effects (SMD range: 0.46 - 0.90). Meta-regression analysis identified an inverse association between TSPO levels in the parietal region and Mini-Mental State Examination scores, a proxy for disease severity, in AD subjects (estimate: -0.11, 95% confidence interval: −0.21 to −0.02; P = 0.024).
Conclusions: Our findings support the association of increased neuroinflammation during the progression of MCI and AD, relative to HCs.

1. Introduction

Alongside the classical pathological hallmarks of Alzheimer's disease (AD), such as misfolded and aggregated proteins, neuroinflammation is thought to be a major driver in disease progression (Calsolaro and Edison, 2016; Heneka et al., 2015). Understanding the role of neuroinflammation in the development of dementia is crucial as a marker for the disease and its progression, and as a target for therapeutic interventions.

Microglia and astrocytes are the predominant mediators of inflammation within the central nervous system. Activated in response to neuropathologies (Meda et al., 1995; Morales et al., 2013), these cells have been prime candidates to investigate the neuroinflammatory process during the disease. Positron emission tomography (PET), together with inflammatory ligands, enable the quantification of levels of inflammation within the brain during dementia progression (Lagarde et al., 2018) and has revealed neuroinflammation as one of the earliest detectable biomarkers in the disease (Calsolaro and Edison, 2016; Okello et al., 2009).

The translocator protein-18 kDa (TSPO) is a transmembrane domain protein has minimal expression within the brain at physiological levels (Banati, 2002). Upon microglial and astrocyte activation TSPO levels are significantly increased (Lavisse et al., 2012; Wilms et al., 2003), supporting TSPO detection as an *in vivo* marker of neuroinflammation. Since the first use of TSPO ligands in PET on AD subjects at the turn of the 21st century (Groom et al., 1995), numerous groups have added further TSPO PET reports (as reviewed in (Lagarde et al., 2018)). However, studies often contain relatively few ($n < 10$) subjects (Femminella et al., 2016; Golla et al., 2015; Groom et al., 1995; Gulyás et al., 2011; Varrone et al., 2013; Wiley et al., 2009), thus limiting the power of analyses.

As such, we performed the first meta-analyses investigating TSPO levels in MCI and AD, in relation to controls, to characterise the spatial progression of neuroinflammatory processes across the brain.

* Corresponding author.
E-mail address: Steven.bradburn@mmu.ac.uk (S. Bradburn).

https://doi.org/10.1016/j.arr.2019.01.002
Received 20 November 2018; Accepted 1 January 2019
Available online 02 January 2019
1568-1637/ © 2019 Elsevier B.V. All rights reserved.

2. Methods

2.1. Search strategy

All meta-analyses were performed according to the Preferred Reporting Items for Systematic Reviews and Meta-analyses (PRISMA) guidelines (Liberati et al., 2009). PubMed and Scopus literature databases were searched, up to 31st July 2018, and were restricted to journal articles written in English.

Search terms used to find potential articles were as follows: ("Positron-emission tomography" OR "PET") AND ("TSPO" OR "Translocator Protein" OR "18 kDa" OR "Neuroinflammation" OR "PK11195" OR "microglia" OR "benzodiazepine") AND ("Alzheimer's disease" OR "dementia" OR "cognitive impairment" OR "MCI" OR "Prodromal"). We also manually searched any included articles for additional relevant references. A standardised review protocol has not been published.

2.2. Eligibility criteria

Studies were included in the meta-analysis based on the following criteria: (1) written in English, (2) measured TSPO binding using PET; (3) participants were stratified into healthy control (HC) and MCI and/or AD groups; (4) performed a regional analysis; (5) TSPO levels were reported.

We excluded studies if they: (1) were of an interventional study design; (2) contained a duplicate study population; (3) did not perform a regional analysis.

2.3. Data extraction

The following data was extracted from each included study: (1) the TSPO ligand used; (2) the outcome used to measure TSPO levels; (3) the number of subjects in each group; (4) the average age of subjects in each group; (5) the proportion of female subjects in each group; (6) the average Mini-Mental State Examination (MMSE) scores of subjects in each group; (7) the average value and standard deviation (SD) for the outcome of TSPO activation in each group.

Where studies reported separate results for both hemispheres (Cagnin et al., 2001; Parbo et al., 2017), results were averaged across hemispheres. When studies reported results in graphical format (Gulyás et al., 2011; Kropholler et al., 2007; Tomasi et al., 2008; Wiley et al., 2009), mean and SD values were estimated by using the measurement tool in Adobe Reader (v.2018.011.20058). One study (Parbo et al., 2017) presented their data as mean with 95% CI in a graphical format, therefore the corresponding author was contacted to request the raw tabulated data, which they kindly provided. One study reported standard error (SE) (Suridjan et al., 2015), as opposed to SD, therefore values were converted to SD using the following formula: $SD = SE \times \sqrt{N}$. Where multiple studies utilised the same study population, we selected the study containing the larger study population for inclusion and excluded the duplicate population. One study (Passamonti et al., 2018) reported combined results for the MCI and AD groups in a graphical format, therefore the corresponding author was contacted for separate results in mean and SD tabulated format, which they kindly provided.

2.4. Quality assessment

The quality of included studies was assessed using the Newcastle-Ottawa quality assessment scale for case-control studies (Wells et al., 2000). A maximum score of 9 can be awarded, whereby studies with ≥ 7 points are generally considered to be of high quality. The criteria for the assessment scale can be found in the Supplementary Material.

2.5. Statistical analysis

Meta-analysis was performed using the *metafor* package in R (Viechtbauer, 2010), when there were ≥2 studies for the same region of interest. Since TSPO levels were determined using different PET ligands and analytical methods, results were converted to standardised mean differences (SMD) between controls and MCI or AD groups. A positive result indicates higher TSPO levels in the cases (AD or MCI), compared to the healthy controls (HC). Results were meta-analysed using a random-effects model and are reported as SMD and 95% confidence intervals (CI).

Statistical heterogeneity across studies was assessed using the I^2 statistic. Subgroup analysis was performed to investigate the potential source of heterogeneity. Specifically, we anticipated the majority of variation to be explained by the type of TSPO ligand used, since second generation TSPO ligands offer superior neuroimaging characteristics, such as increased sensitivity and signal to noise ratios, compared to the initial generation (Alam et al., 2017). We therefore stratified studies in two: 1st generation ([11C]PK11195 or [11C](*R*)-PK11195) or 2nd generation ([11C]DAA1106, [11C]Vinpocetine, [11C]PBR28, [18 F]FEDAA1106, [18 F]DPA-714, [18 F]FEPPA, [18 F]FEMPA, [11C]DPA713) TSPO ligands. We also performed subgroup analysis based on study quality scores (< 7 points / ≥ 7 points).

Sensitivity analysis was conducted on those regions which reached statistical significance to assess the robustness of the result. Specifically, the leave-1-out method was applied which repeated the random effects model by leaving out one study at a time. The results of this analysis are reported as the number of studies which can be removed without affecting the significance of the model.

Mixed-effects meta-regressions were performed, through the *rma* function, when the number of studies permitted (≥ 10 studies) to determine the relationship between SMD and patient MMSE scores, a proxy of disease severity.

Publication bias was tested when the number of studies permitted (> 2 studies), through the Egger regression test. Models that were significant after publication bias testing were further entered into trim-and-fill analysis. This method aims to identify and correct for funnel plot asymmetry by imputing possible missing studies.

3. Results

3.1. Study selection

Following the literature searches, 528 articles were returned, of which 455 were excluded based on title and abstract suitability (Fig. 1). After removal of duplicate results, the full text of 40 articles was examined. Following this, 13 articles were excluded because they did not meet our inclusion criteria, and 27 articles were eligible for inclusion in the meta-analyses.

One article (Yokokura et al., 2017) reported results from two independent studies using different TSPO ligands, therefore these were treated as two separate studies. Overall, 28 studies were meta-analysed, of which 13 and 23 studies contained MCI and AD groups, respectively.

3.2. Study characteristics

The overall study characteristics of interest, including the type of PET ligand used, outcome, number of subjects, age of subjects, proportion of female subjects and subject MMSE scores for each included study is presented in Table 1. Quality scores of the included studies ranged between 4–9 points (Table A.1), with the majority being of high quality (≥ 7 points).

In total, there were 37 regions with data available for meta-analysis. These regions are defined as: amygdala, anterior cingulate (including: cortex and gyrus), caudate, cerebellum, cortex (including: averaged cerebral cortex, cortical and whole cortex), entorhinal, frontal

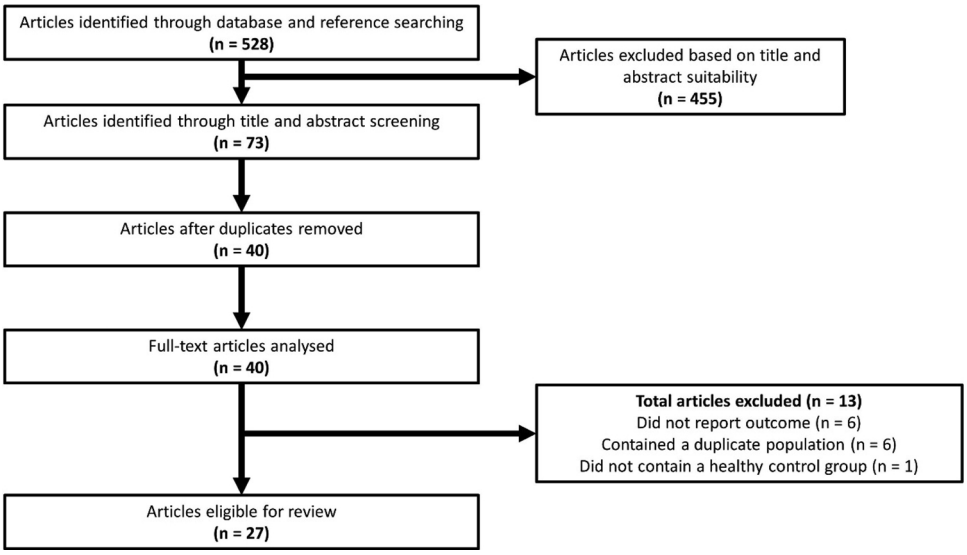

Fig. 1. Flowchart illustrating the literature search strategy.

(including: cortex and lobe), gray matter, hippocampus, inferior and middle temporal (including: gyri and cortex), insula, lateral temporal, lingual gyrus, medial temporal (including: region, cortex, lobe, pole), midbrain, middle frontal (including: cortex and gyrus), occipital (including: cortex, lobe and lateral region), orbitofrontal, pallidum, parahippocampal (including: cortex and gyrus), parietal (including: lobe, cortex, and lateral), inferior parietal (including: lobule and cortex), superior parietal (including: cortex and gyrus), posterior cingulate (including: gyrus and cortex), posterior temporal (including: lobe and cortex), precuneus, prefrontal cortex (including: dorsolateral and lateral), pons, putamen, sensorimotor cortex, striatum, superior frontal (including cortex and gyrus), superior temporal (including cortex and gyrus), temporal (including: cortex and lobe), thalamus, white matter (including: averaged cerebral white matter), whole brain.

3.3. Meta-analysis between HC and AD subjects

For the comparison between the HC and AD groups, 36 regions were available for meta-analysis, of which 27 regions had significantly higher TSPO levels in the AD subjects compared to the HC subjects (Fig. 2, Table 2). The largest effects were seen in cortical regions, especially within fronto-temporal regions (Fig. 2, Table 2). There were no differences in the putamen, cortex, lingual gyrus, caudate, insula, midbrain, sensorimotor cortex, white matter or gray matter.

Sensitivity analysis through leave-1-out found the cerebellum, orbitofrontal cortex, pallidum, pons, striatum, entorhinal and lateral temporal region model effects were affected by one or more study exclusions (Table A.2).

Publication bias was evident in the amygdala, anterior cingulate, posterior cingulate, middle frontal, prefrontal cortex, superior frontal, superior parietal, precuneus, entorhinal, inferior and middle temporal and parahippocampal regions (Table A.2). Apart from the amygdala model, imputing potential missing studies through trim-and-fill analysis failed to change these overall model effects (Table A.2).

Significant study heterogeneity was detected in the majority of models (Table 2). To investigate potential sources of heterogeneity, subgrouping was performed for study quality (< 7 / ≥ 7 quality score) and the type of TSPO ligand used (1^{st} generation / 2^{nd} generation). Heterogeneity in the anterior cingulate, caudate, superior frontal, parietal, putamen, hippocampus, inferior and middle temporal, lateral temporal and thalamus models were reduced when stratified by TSPO ligand type (Table A.3). Further, when stratified by study quality, heterogeneity within the anterior cingulate, posterior cingulate, cerebellum, cortex, occipital, parietal, precuneus, putamen, hippocampus, inferior and middle temporal, parahippocampal and thalamus region models were reduced (Table A.4).

Meta-regression analysis was performed in models with $\geq$ 10 included studies to determine the association of AD subject MMSE scores with SMD effect sizes. There was no significant association in the anterior cingulate (estimate: -0.03; 95% CI: -0.19 - 0.13; P = 0.678), posterior cingulate (estimate: -0.10; 95% CI: -0.22 - 0.01; P = 0.086), cerebellum (estimate: -0.09; 95% CI: -0.21 - 0.04; P = 0.189), occipital (estimate: -0.11; 95% CI: -0.23 - 0.01; P = 0.082), thalamus (estimate: -0.03; 95% CI: -0.15 - 0.09; P = 0.558) or hippocampus (estimate: -0.02; 95% CI: -0.18 - 0.13; P = 0.769) region models. However, there was a negative association between MMSE scores and SMD effect sizes in the parietal region model (estimate: -0.11, 95% CI: -0.21 to -0.02; P = 0.024, Fig. 3).

3.4. Meta-analysis between HC and MCI subjects

There were 22 regions of interest meta-analysed for the comparisons between MCI and HC subjects (Fig. 2, Table 3). From these, the MCI subjects had significantly more TSPO levels within the anterior cingulate, posterior cingulate, frontal, occipital, inferior parietal, precuneus, temporal, hippocampus, lateral temporal, medial temporal, thalamus and whole brain regions compared to HC subjects (Fig. 2, Table 3). There were no differences in the amygdala, cerebellum, prefrontal cortex, superior parietal, sensorimotor cortex, striatum, entorhinal, inferior and middle temporal, parahippocampal and superior temporal regions between the groups (Fig. 2, Table 3).

Leave-1-out analysis was performed on the significant models and found that the anterior cingulate, lateral temporal and whole brain models were dependent on one or more studies included in the model (Table A.5). The posterior cingulate, frontal, occipital, parietal, precuneus, temporal, hippocampus, medial temporal and thalamus regions were unaffected by single study exclusions.

Publication bias was only evident in the amygdala and striatum models (Table A.5). Despite this, trim-and-fill analysis failed to impute any missing studies (Table A.5).

Significant study heterogeneity was only evident in the amygdala model (Table 3). However, this heterogeneity was not explained by the type of TSPO ligand used (Table A.6) or the quality of the included studies (Table A.7).

Meta-regression was only performed on the posterior cingulate, which failed to report an association between patient MMSE scores and

Table 1
Characteristics of included studies.

Study	Ligand	Outcome	Subjects (n)			Age (mean & SD)			Female (%)			MMSE (mean & SD)		
			HC	MCI	AD	HC	MCI	AD	HC	MCI	AD	HC	MCI	AD
Groom et al., 1995	[11C]PK11195	Normalised binding	7	N/A	8	42-78[a]	N/A	69-80[a]	Un	N/A	63	Un	N/A	6-23[a]
Cagnin et al., 2001	[11C](R)-PK11195	Binding potential	15	N/A	8	57 (21)[b]	N/A	65.1 (6.1)	47	N/A	50	Un	N/A	17 (6.4)
Kropholler et al., 2007	[11C](R)-PK11195	Binding potential	10	10	9	70 (6)	74 (6)	71 (6)	40	40	33	29 (1)	26 (1)	22 (3)
Edison et al., 2008	[11C](R)-PK11195	Binding potential	10	N/A	13	64.2 (5.5)	N/A	65.6 (4.6)	40	N/A	38	30	N/A	21.2 (3.9)
Tomasi et al., 2008	[11C](R)-PK11195	Binding potential	10	N/A	10	Un	N/A	Un	Un	N/A	Un	Un	N/A	Un
Yasuno et al., 2008	[11C]DAA1106	Binding potential	10	N/A	10	67.9 (5)	N/A	70.2 (7.4)	30	N/A	50	29.7 (0.67)	N/A	20.6 (2.67)
Okello et al., 2009	[11C](R)-PK11195	Binding potential	10	13	N/A[c]	60.2 (9.3)	66.6 (9.6)	N/A[c]	40	36	N/A[c]	29.9 (0.3)	27.7 (1.5)	N/A[c]
Wiley et al., 2009	[11C](R)-PK11195	Region of interest to subcortical white matter ratio (atrophy corrected)	5	6	6	72.0 (5.9)	71.8 (8.5)	76.5 (10.5)	40	33	33	29.4 (0.9)	28.7 (1.0)	19.3 (4.8)
Gulyás et al., 2011	[11C]Vinpocetine	Standardized uptake values	6	N/A	6	67.3 (7.6)	N/A	73.4 (6.2)	0	N/A	50	Un	N/A	Un
Yokokura et al., 2011	[11C](R)-PK11195	Binding potential	10	N/A	11	Un	N/A	70.6 (6.4)	Un	N/A	45	Un	N/A	21.5 (3.5)
Yasuno et al., 2012	[11C]DAA1106	Binding potential	10	7	N/A[d]	67.9 (5)	67.1 (10.7)	N/A[d]	30	43	N/A[d]	29.7 (0.7)	28.6 (1.3)	N/A[d]
Kreisl et al., 2013	[11C]PBR28	Distribution volume corrected for free fraction of radioligand in plasma (partial volume corrected)	13	10	19	62.9 (6.4)	72.6 (9.7)	63.1 (8.8)	31	40	42	29.8 (0.4)	27.5 (2)	20.3 (4.2)
Schuitemaker et al., 2013	[11C](R)-PK11195	Binding potential	21	10	19	68 (8)	72 (6)	69 (8)	38	30	42	29 (1)	26 (1)	23 (3)
Varrone et al., 2013	[18 F]FEDAA1106	Binding potential	7	N/A	9	68 (3)	N/A	69 (4)	29	N/A	33	29 (1)	N/A	25 (3)
Fan et al., 2015	[11C](R)-PK11195	Binding potential	8	10	10	65.5 (5.5)	67.7 (7.7)	66.3 (6.1)	50	50	60	30	28.2 (1.8)	20.5 (4.2)
Golla et al., 2015	[18 F]DPA-714	Binding potential	6	N/A	9	64.5 (5.5)	N/A	73.6 (8.4)	83	N/A	44	28.8 (0.8)	N/A	24.6 (2.8)
Lyoo et al., 2015	[11C]PBR28	Standardized uptake value ratio	21	11	25	55.1 (15.3)	72.2 (9.3)	63.0 (8.3)	29	36	56	Un	Un	Un
Suridjan et al., 2015	[18 F]FEPPA	Total distribution volume (partial volume error corrected)	21	N/A	18	61.3 (9.9)	N/A	68.3 (9.4)	57	N/A	48	29.4 (0.9)	N/A	17.5 (7)
Varrone et al., 2015	[18 F]FEMPA	Total distribution volume	7	N/A	10	64 (7)	N/A	67 (7)	57	N/A	50	29.3 (1.0)	N/A	25.5 (2.5)
Femminella et al., 2016	[11C](R)-PK11195	Binding potential	8	N/A	8	65.9 (6.2)	N/A	66.2 (6.4)	25	N/A	38	29.4 (0.9)	N/A	19 (5.3)
Hamelin et al., 2016	[18 F]DPA-714	Standardized uptake value ratio	20	34	24	68.2 (8.4)	67.8 (9.1)	68.3 (12.1)	75	58	69	29.5 (0.6)	24.1 (2.8)	15.8 (4.5)
Knezevic et al., 2017	[18 F]FEPPA	Standardized uptake value ratios (partial volume error corrected)	14	11	N/A	67.1 (6.5)	71.9 (5.3)	N/A	64	55	N/A	29.3 (1.3)	27.3 (2.0)	N/A
Kreisl et al., 2017	[11C]PBR28	Standardized uptake value ratio	15	N/A	11	63.7 (4.7)	N/A	65.6 (7.3)	20	N/A	45	29.9 (0.4)	N/A	21.5 (4.7)
Parbo et al., 2017	[11C](R)-PK11195	Binding potential	10	26	N/A	68.3 (6.6)	73.3 (6.2)	N/A	60	35	N/A	29 (25-30)[e]	27 (23-30)[e]	N/A
Yokokura et al., 2017	[11C]DPA713	Binding potential	12	N/A	7	71.6 (2.6)	N/A	69.3 (7.4)	58	N/A	86	28.3 (1.1)	N/A	19.4 (2.9)
Yokokura et al., 2017	[11C](R)-PK11195	Binding potential	10	N/A	10	72.2 (8.1)	N/A	70.8 (6.7)	60	N/A	50	29.5 (1.0)	N/A	22.1 (3.5)
Fan et al., 2018	[11C]PBR28	Impulse response function	9	13	N/A	65.4 (7.5)	70.9 (8.1)	N/A	Un	Un	N/A	29.4 (1.0)	26.8 (2.9)	N/A
Passamonti et al., 2018	[11C]PK11195	Binding potential	13	7	9	68.0 (5.5)	70.3 (5.0)	67.4 (10.5)	62	71	22	28.7 (1.0)	26.6 (1.8)	24.6 (3.5)

Key: Un = Unknown. [a] Range. [b] Median and inter-quartile range. [c] Removed from analysis because they contained the same subjects as in Edison et al., 2008. [d] Removed from analysis because they contained the same subjects as in Yasuno et al., 2008. [e] Median and range.

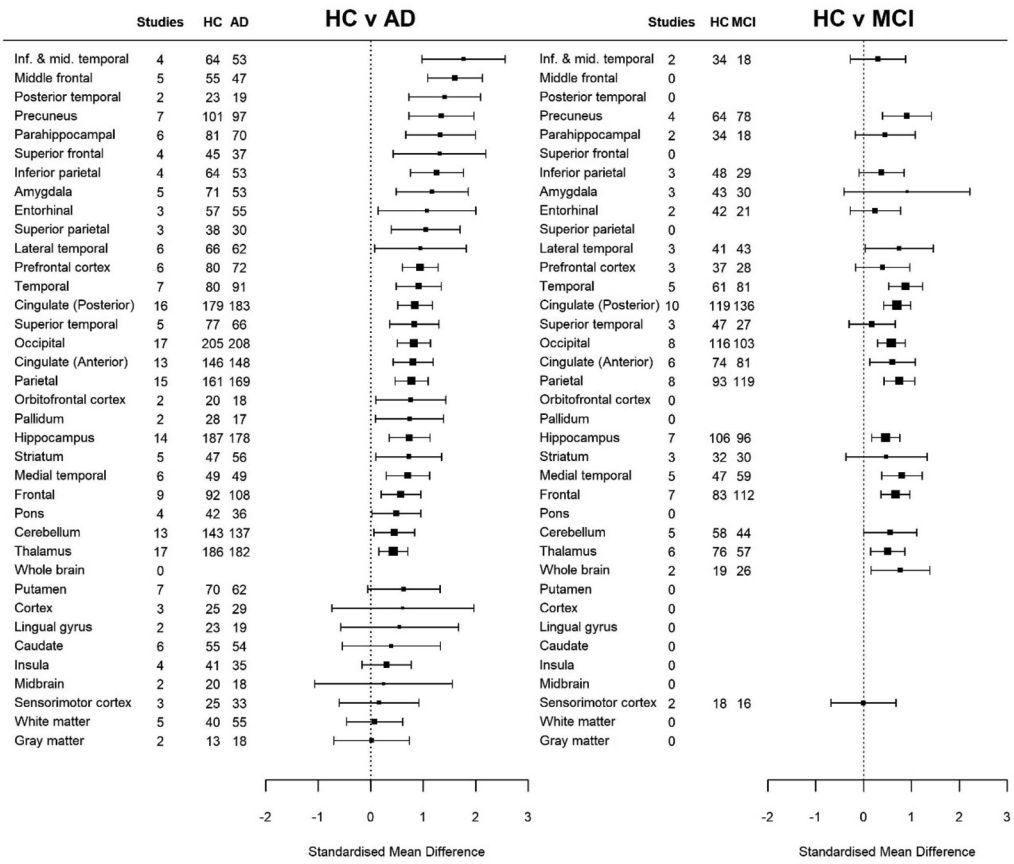

Fig. 2. Overall standardised mean difference for each region of interest model in the comparison between HC and AD subjects (left) and HC and MCI subjects (right). Results are organised by regional effect size in the HC and AD analysis. Detailed model reports are presented in Tables 2 and 3.

SMD values (estimate: -0.06; 95% CI: -0.26 - 0.14; P = 0.536).

4. Discussion

The present meta-analysis contained 28 studies covering 37 different brain regions of interest for levels of neuroinflammation in AD and MCI, relative to controls. Levels of neuroinflammation were higher and more disperse in AD, whereas only modest levels were detected in MCI, primarily within the neocortex. Further, in studies concerning AD subjects, effect sizes were associated with disease severity (MMSE scores) in the parietal region. Collectively, these results are in agreement with recent reports of an increase in neuroinflammation with disease progression (Calsolaro and Edison, 2016; Fan et al., 2017).

The predominant hypothesis suggests levels of neuroinflammation peaks early on, possibly reflecting an initial anti-inflammatory response, followed by a second peak during conversion from MCI to AD, which may indicate a pro-inflammatory shift (Calsolaro and Edison, 2016; Fan et al., 2017; Hamelin et al., 2016). This complex relationship may be related to the microglial reaction following the deposition and propagation of amyloid and hyperphosphorylated tau pathologies, which can be internalised by and activate glia (Meda et al., 1995; Morales et al., 2013).

Evidence from PET studies utilising TSPO and amyloid or tau ligands have shown strong inter-relationships of neuroinflammation with amyloid levels in early MCI (Dani et al., 2018; Fan et al., 2017; Hamelin et al., 2016; Parbo et al., 2018, 2017), with little (Dani et al., 2018) or no correlations (Parbo et al., 2018) with tau levels. Thus, the inflammatory peak during the prodromal phase may reflect the anti-inflammatory response of microglia to amyloid. Amyloid deposition is initially seen throughout the neocortex, before expanding ventrally into the allocortex, midbrain, brainstem and eventually into cerebellar areas (Thal et al., 2002). This pattern is in alignment with our findings in the MCI subjects, where increased neuroinflammation was seen within cortical regions associated with early amyloid deposition (e.g. frontal, occipital, parietal, temporal), whereas regions generally associated with later stages were less affected (e.g. striatum and cerebellum).

On the other hand, neuroinflammation and tau associations are much closely aligned in AD, than they are in MCI (Dani et al., 2018). Histological analyses also support this linear association of microgliosis with tau tangle burden during disease severity (Serrano-Pozo et al., 2011). Our results corroborate the spatial propagation of tau during AD with all of the temporal regions having high effects of neuroinflammation, a region dominated with exacerbated tau aggregation during the disease course (Braak et al., 2006). Collectively therefore, the spatial pattern of neuroinflammation during AD may be a reaction to initial amyloid deposition in the earlier phases, with a second hit during later tau spreading.

A conceivable weakness of current PET studies targeting TSPO is that the ligands used can only indicate the activation level of the regional analysis, rather, they are unable to differentiate between pro- and anti-inflammatory states of microglia and astrocytes. Future developments of ligands that can discriminate these inflammatory states, such as the promising recent insights into P2Y12R and P2 × 7R receptor targeting (Beaino et al., 2017), will be vital in elucidating these associations with disease progression and further aid with potential therapy monitoring (Janssen et al., 2018).

Another noteworthy finding from our analyses is the cerebellum as a region with significantly increased TSPO binding in the AD subjects. The cerebellum is often selected as a reference region during TSPO PET image analysis (Groom et al., 1995; Hamelin et al., 2016; Kreisl et al., 2017; Kropholler et al., 2007; Lyoo et al., 2015), mainly due to the belief that this region is relatively spared from AD pathology. Based on

Table 2
Random effects meta-analyses results, stratified by region of interest, between HC and AD subjects.

		Subjects			Overall effect		Heterogeneity	
Region	Number of studies	HC	AD	SMD [95% CI]	Z	P	I^2	P
Amygdala	5	71	53	1.17 [0.48 - 1.85]	3.34	*0.001*	65.5%	*0.017*
Cingulate (Anterior)	13	146	148	0.81 [0.42 - 1.19]	4.14	*< 0.001*	57.3%	*0.006*
Cingulate (Posterior)	16	179	183	0.84 [0.51 - 1.17]	4.98	*< 0.001*	53.4%	*0.004*
Caudate	6	55	54	0.39 [-0.54 - 1.32]	0.82	0.413	81.1%	*0.001*
Cerebellum	13	143	137	0.45 [0.06 - 0.83]	2.27	*0.023*	57.1%	*0.006*
Cortex	3	25	29	0.61 [-0.74 - 1.96]	0.88	0.376	81.3%	*0.006*
Frontal	9	92	108	0.57 [0.19 - 0.95]	2.96	*0.003*	37.1%	0.088
Middle frontal	5	55	47	1.60 [1.08 - 2.12]	6.04	*< 0.001*	23.0%	0.236
Orbitofrontal cortex	2	20	18	0.76 [0.10 - 1.43]	2.24	*0.025*	0.0%	0.853
Prefrontal cortex	6	80	72	0.94 [0.60 - 1.28]	5.38	*< 0.001*	0.0%	0.416
Superior frontal	4	45	37	1.31 [0.42 - 2.19]	2.90	*0.004*	68.6%	*0.033*
Grey matter	2	13	18	0.02 [-0.70 - 0.74]	0.05	0.961	0.0%	0.396
Insula	4	41	35	0.30 [-0.17 - 0.77]	1.26	0.209	0.0%	0.562
Midbrain	2	20	18	0.24 [-1.07 - 1.55]	0.36	0.716	73.9%	0.050
Occipital	17	205	208	0.82 [0.50 - 1.14]	5.06	*< 0.001*	55.5%	*0.003*
Lingual gyrus	2	23	19	0.55 [-0.57 - 1.67]	0.96	0.339	67.9%	0.078
Pallidum	2	28	17	0.74 [0.09 - 1.39]	2.23	*0.026*	6.7%	0.301
Parietal	15	161	169	0.77 [0.46 - 1.09]	4.81	*< 0.001*	44.1%	*0.028*
Inferior parietal	4	64	53	1.26 [0.75 - 1.76]	4.87	*< 0.001*	32.5%	0.251
Superior parietal	3	38	30	1.05 [0.39 - 1.70]	3.13	*0.002*	37.0%	0.202
Precuneus	7	101	97	1.34 [0.72 - 1.97]	4.24	*< 0.001*	72.8%	*0.002*
Pons	4	42	36	0.49 [0.02 - 0.95]	2.06	*0.039*	0.0%	0.470
Putamen	7	70	62	0.63 [-0.06 - 1.32]	1.79	0.074	70.7%	*0.005*
Sensorimotor cortex	3	25	33	0.16 [-0.60 - 0.91]	0.41	0.684	46.0%	0.162
Striatum	5	47	56	0.72 [0.10 - 1.35]	2.26	*0.024*	54.9%	0.068
Temporal	7	80	91	0.92 [0.49 - 1.34]	4.18	*< 0.001*	40.0%	0.107
Entorhinal	3	57	55	1.07 [0.14 - 2.00]	2.25	*0.024*	80.3%	*0.018*
Hippocampus	14	187	178	0.74 [0.35 - 1.13]	3.72	*< 0.001*	66.6%	*0.001*
Inferior and middle temporal	4	64	53	1.76 [0.97 - 2.56]	4.36	*< 0.001*	67.2%	*0.015*
Lateral temporal	6	66	62	0.95 [0.08 - 1.82]	2.13	*0.033*	79.8%	*0.001*
Medial temporal	6	49	49	0.71 [0.29 - 1.12]	3.33	*0.001*	0.0%	0.401
Parahippocampal	6	81	70	1.33 [0.67 - 1.99]	3.93	*< 0.001*	68.2%	*0.012*
Posterior temporal	2	23	19	1.41 [0.73 - 2.09]	4.04	*< 0.001*	0.0%	0.464
Superior temporal	5	77	66	0.83 [0.36 - 1.30]	3.46	*0.001*	42.6%	0.137
Thalamus	17	186	182	0.43 [0.16 - 0.70]	3.07	*0.002*	37.7%	*0.040*
White matter	5	40	55	0.07 [-0.46 - 0.61]	0.27	0.791	37.9%	0.150

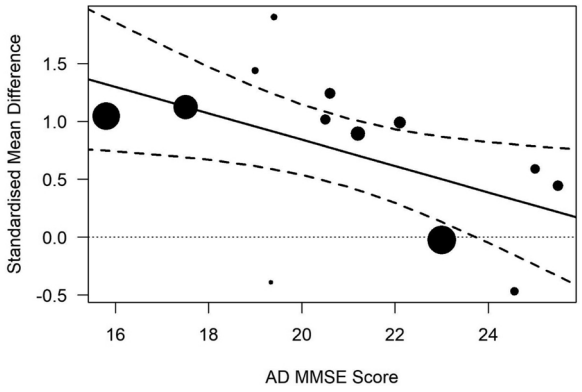

Fig. 3. Scatterplot demonstrating the association of AD MMSE score with standardised mean difference values in the parietal region. The size of study points is proportional to their precision. Lines presented are average predicted values with 95% confidence intervals (dashed lines).

our findings, we would not recommend this structure as an appropriate reference region. For an alternative reference during image analysis, our results suggest the caudate or white matter may be a better alternative to the cerebellum. The lack of TSPO signal differences in the caudate, for example, is also corroborated in a an early report describing no difference in the number of microglia between control and AD caudate brain tissue (Falke et al., 2000).

Despite the strengths of the current investigation, it is important to address some important limitations. One challenge is that some of the regional analysis contained relatively few studies, especially involving MCI subjects, which can restrict the power of these analyses and limit publication bias detection. Clearly, additional studies, particularly involving MCI subjects covering more regions are warranted. Additionally, the included studies measured TSPO levels through a variety of analytical methods and different ligands. We did, however, anticipate such heterogeneity by applying random-effect models throughout and performing *post-hoc* subgroup analyses.

Collectively, our findings support the observation of increased neuroinflammation during MCI and AD progression. Further work concerning longitudinal PET analysis and additional ligand development is needed in the prodromal AD phases to fully understand the spatio-temporal sequence of neuroinflammatory events.

Study funding

This research did not receive any specific grant from funding agencies in the public, commercial, or not-for-profit sectors.

Competing interests

None.

Acknowledgements

We would like to thank Dr's Parbo and Passamonti for kindly agreeing to and providing the requested data to enable their study inclusion within the analysis.

Table 3
Random effects meta-analyses results, stratified by region of interest, between HC and MCI subjects.

		Subjects			Overall effect		Heterogeneity	
Region	Number of studies	HC	MCI	SMD [95% CI]	Z	P	I^2	P
Amygdala	3	43	30	0.90 [-0.41 - 2.21]	1.35	0.176	83.6%	*0.001*
Cingulate (Anterior)	6	74	81	0.60 [0.13 - 1.08]	2.48	*0.013*	46.9%	0.095
Cingulate (Posterior)	10	119	136	0.70 [0.42 - 0.98]	4.86	*< 0.001*	10.6%	0.412
Cerebellum	5	58	44	0.55 [-0.00 - 1.11]	1.95	0.051	42.2%	0.149
Frontal	7	83	112	0.66 [0.36 - 0.97]	4.31	*< 0.001*	0.0%	0.653
Prefrontal cortex	3	37	28	0.40 [-0.17 - 0.97]	1.38	0.168	21.3%	0.270
Occipital	8	116	103	0.58 [0.29 - 0.86]	3.94	*< 0.001*	3.2%	0.471
Parietal	8	93	119	0.75 [0.42 - 1.07]	4.53	*< 0.001*	15.2%	0.285
Inferior parietal	3	48	29	0.37 [-0.09 - 0.84]	1.56	0.118	0.0%	0.696
Precuneus	4	64	78	0.90 [0.39 - 1.41]	3.47	*< 0.001*	45.1%	0.142
Sensorimotor cortex	2	18	16	0.00 [-0.68 - 0.68]	−0.01	0.991	0.0%	0.459
Striatum	3	32	30	0.48 [-0.37 - 1.32]	1.11	0.269	61.2%	0.082
Temporal	5	61	81	0.87 [0.52 - 1.23]	4.87	*< 0.001*	0.0%	0.443
Entorhinal	2	42	21	0.24 [-0.28 - 0.77]	0.91	0.365	0.0%	0.548
Hippocampus	7	106	96	0.46 [0.17 - 0.76]	3.12	*0.002*	0.0%	0.487
Inferior and middle temporal	2	34	18	0.30 [-0.28 - 0.88]	1.02	0.309	0.0%	0.384
Lateral temporal	3	41	43	0.74 [0.04 - 1.45]	2.06	*0.040*	52.3%	0.123
Medial temporal	5	47	59	0.80 [0.38 - 1.22]	3.75	*< 0.001*	0.0%	0.545
Parahippocampal	2	34	18	0.45 [-0.17 - 1.08]	1.41	0.157	12.1%	0.286
Superior temporal	3	47	27	0.18 [-0.31 - 0.66]	0.71	0.475	0.0%	0.318
Thalamus	6	76	57	0.50 [0.14 - 0.86]	2.74	*0.006*	0.0%	0.550
Whole brain	2	19	26	0.77 [0.15 -1.38]	2.44	*0.015*	0.0%	0.540

Appendix A. Supplementary data

Supplementary material related to this article can be found, in the online version, at doi:https://doi.org/10.1016/j.arr.2019.01.002.

References

Alam, M.M., Lee, J., Lee, S.-Y., 2017. Recent progress in the development of TSPO PET ligands for neuroinflammation imaging in neurological diseases. Nucl. Med. Mol. Imaging 51, 283–296. https://doi.org/10.1007/s13139-017-0475-8.

Banati, R.B., 2002. Visualising microglial activation in vivo. Glia 40, 206–217. https://doi.org/10.1002/glia.10144.

Beaino, W., Janssen, B., Kooij, G., van der Pol, S.M.A., van Het Hof, B., van Horssen, J., Windhorst, A.D., de Vries, H.E., 2017. Purinergic receptors P2Y12R and P2X7R: potential targets for PET imaging of microglia phenotypes in multiple sclerosis. J. Neuroinflammation 14. https://doi.org/10.1186/s12974-017-1034-z.

Braak, H., Alafuzoff, I., Arzberger, T., Kretzschmar, H., Del Tredici, K., 2006. Staging of Alzheimer disease-associated neurofibrillary pathology using paraffin sections and immunocytochemistry. Acta Neuropathol. 112, 389–404. https://doi.org/10.1007/s00401-006-0127-z.

Cagnin, A., Brooks, D.J., Kennedy, A.M., Gunn, R.N., Myers, R., Turkheimer, F.E., Jones, T., Banati, R.B., 2001. In-vivo measurement of activated microglia in dementia. Lancet 358, 461–467. https://doi.org/10.1016/S0140-6736(01)05625-2.

Calsolaro, V., Edison, P., 2016. Neuroinflammation in Alzheimer's disease: current evidence and future directions. Alzheimer's & Dementia 12, 719–732. https://doi.org/10.1016/j.jalz.2016.02.010.

Dani, M., Wood, M., Mizoguchi, R., Fan, Z., Walker, Z., Morgan, R., Hinz, R., Biju, M., Kuruvilla, T., Brooks, D.J., Edison, P., 2018. Microglial activation correlates in vivo with both tau and amyloid in Alzheimer's disease. Brain. https://doi.org/10.1093/brain/awy188.

Edison, P., Archer, H.A., Gerhard, A., Hinz, R., Pavese, N., Turkheimer, F.E., Hammers, A., Tai, Y.F., Fox, N., Kennedy, A., Rossor, M., Brooks, D.J., 2008. Microglia, amyloid, and cognition in Alzheimer's disease: an [11C](R)PK11195-PET and [11C]PIB-PET study. Neurobiol. Dis. 32, 412–419. https://doi.org/10.1016/j.nbd.2008.08.001.

Falke, E., Han, L.-Y., Arnold, S.E., 2000. Absence of neurodegeneration in the thalamus and caudate of elderly patients with schizophrenia. Psychiatry Res. 93, 103–110. https://doi.org/10.1016/S0165-1781(00)00104-9.

Fan, Z., Aman, Y., Ahmed, I., Chetelat, G., Landeau, B., Chaudhuri, K.R., Brooks, D.J., Edison, P., 2015. Influence of microglial activation on neuronal function in Alzheimer's and Parkinson's disease dementia. Alzheimer's & Dementia: J. Alzheimer's Assoc. 11, 608–621. https://doi.org/10.1016/j.jalz.2014.06.016. e7.

Fan, Z., Brooks, D.J., Okello, A., Edison, P., 2017. An early and late peak in microglial activation in Alzheimer's disease trajectory. Brain 140, 792–803. https://doi.org/10.1093/brain/aww349.

Fan, Z., Dani, M., Femminella, G.D., Wood, M., Calsolaro, V., Veronese, M., Turkheimer, F., Gentleman, S., Brooks, D.J., Hinz, R., Edison, P., 2018. Parametric mapping using spectral analysis for 11C-PBR28 PET reveals neuroinflammation in mild cognitive impairment subjects. Eur. J. Nucl. Med. Mol. Imaging 45, 1432–1441. https://doi.org/10.1007/s00259-018-3984-5.

Femminella, G.D., Ninan, S., Atkinson, R., Fan, Z., Brooks, D.J., Edison, P., 2016. Does microglial activation influence hippocampal volume and neuronal function in Alzheimer's disease and parkinson's disease dementia? J. Alzheimers Dis. 51, 1275–1289. https://doi.org/10.3233/JAD-150827.

Golla, S.S.V., Boellaard, R., Oikonen, V., Hoffmann, A., van Berckel, B.N.M., Windhorst, A.D., Virta, J., Haaparanta-Solin, M., Luoto, P., Savisto, N., Solin, O., Valencia, R., Thiele, A., Eriksson, J., Schuit, R.C., Lammertsma, A.A., Rinne, J.O., 2015. Quantification of [18F]DPA-714 binding in the human brain: initial studies in healthy controls and Alzheimer's disease patients. J. Cereb. Blood Flow Metab. 35, 766–772. https://doi.org/10.1038/jcbfm.2014.261.

Groom, G.N., Junck, L., Foster, N.L., Frey, K.A., Kuhl, D.E., 1995. PET of peripheral benzodiazepine binding sites in the microgliosis of Alzheimer's disease. J. Nucl. Med. 36, 2207–2210.

Gulyás, B., Vas, A., Tóth, M., Takano, A., Varrone, A., Cselényi, Z., Schain, M., Mattsson, P., Halldin, C., 2011. Age and disease related changes in the translocator protein (TSPO) system in the human brain: positron emission tomography measurements with [11C]vinpocetine. Neuroimage 56, 1111–1121. https://doi.org/10.1016/j.neuroimage.2011.02.020.

Hamelin, L., Lagarde, J., Dorothée, G., Leroy, C., Labit, M., Comley, R.A., de Souza, L.C., Corne, H., Dauphinot, L., Bertoux, M., Dubois, B., Gervais, P., Colliot, O., Potier, M.C., Bottlaender, M., Sarazin, M., Clinical IMABio3 team, 2016. Early and protective microglial activation in Alzheimer's disease: a prospective study using 18F-DPA-714 PET imaging. Brain 139, 1252–1264. https://doi.org/10.1093/brain/aww017.

Heneka, M.T., Carson, M.J., El Khoury, J., Landreth, G.E., Brosseron, F., Feinstein, D.L., Jacobs, A.H., Wyss-Coray, T., Vitorica, J., Ransohoff, R.M., Herrup, K., Frautschy, S.A., Finsen, B., Brown, G.C., Verkhratsky, A., Yamanaka, K., Koistinaho, J., Latz, E., Halle, A., Petzold, G.C., Town, T., Morgan, D., Shinohara, M.L., Perry, V.H., Holmes, C., Bazan, N.G., Brooks, D.J., Hunot, S., Joseph, B., Deigendesch, N., Garaschuk, O., Boddeke, E., Dinarello, C.A., Breitner, J.C., Cole, G.M., Golenbock, D.T., Kummer, M.P., 2015. Neuroinflammation in Alzheimer's disease. Lancet Neurol. 14, 388–405. https://doi.org/10.1016/S1474-4422(15)70016-5.

Janssen, B., Vugts, D., Windhorst, A., Mach, R., Janssen, B., Vugts, D.J., Windhorst, A.D., Mach, R.H., 2018. PET imaging of microglial activation—beyond targeting TSPO. Molecules 23, 607. https://doi.org/10.3390/molecules23030607.

Knezevic, D., Verhoeff, N.P.L., Hafizi, S., Strafella, A.P., Graff-Guerrero, A., Rajji, T., Pollock, B.G., Houle, S., Rusjan, P.M., Mizrahi, R., 2017. Imaging microglial activation and amyloid burden in amnestic mild cognitive impairment. J. Cereb. Blood Flow Metab., 271678X17741395. https://doi.org/10.1177/0271678X17741395.

Kreisl, W.C., Lyoo, C.H., McGwier, M., Snow, J., Jenko, K.J., Kimura, N., Corona, W., Morse, C.L., Zoghbi, S.S., Pike, V.W., McMahon, F.J., Turner, R.S., Innis, R.B., Biomarkers Consortium PET Radioligand Project Team, 2013. In vivo radioligand binding to translocator protein correlates with severity of Alzheimer's disease. Brain 136, 2228–2238. https://doi.org/10.1093/brain/awt145.

Kreisl, W.C., Lyoo, C.H., Liow, J.-S., Snow, J., Page, E., Jenko, K.J., Morse, C.L., Zoghbi, S.S., Pike, V.W., Turner, R.S., Innis, R.B., 2017. Distinct patterns of increased translocator protein in posterior cortical atrophy and amnestic Alzheimer's disease. Neurobiol. Aging 51, 132–140. https://doi.org/10.1016/j.neurobiolaging.2016.12.006.

Kropholler, M.A., Boellaard, R., van Berckel, B.N.M., Schuitemaker, A., Kloet, R.W., Lubberink, M.J., Jonker, C., Scheltens, P., Lammertsma, A.A., 2007. Evaluation of reference regions for (R)-[(11)C]PK11195 studies in Alzheimer's disease and mild cognitive impairment. J. Cereb. Blood Flow Metab. 27, 1965–1974. https://doi.org/10.1038/sj.jcbfm.9600488.

Lagarde, J., Sarazin, M., Bottlaender, M., 2018. In vivo PET imaging of neuroinflammation in Alzheimer's disease. J. Neural Transm. 125, 847–867. https://doi.org/10.1007/s00702-017-1731-x.

Lavisse, S., Guillermier, M., Hérard, A.-S., Petit, F., Delahaye, M., Van Camp, N., Ben Haim, L., Lebon, V., Remy, P., Dollé, F., Delzescaux, T., Bonvento, G., Hantraye, P., Escartin, C., 2012. Reactive astrocytes overexpress TSPO and are detected by TSPO positron emission tomography imaging. J. Neurosci. 32, 10809–10818. https://doi.org/10.1523/JNEUROSCI.1487-12.2012.

Liberati, A., Altman, D.G., Tetzlaff, J., Mulrow, C., Gøtzsche, P.C., Ioannidis, J.P.A., Clarke, M., Devereaux, P.J., Kleijnen, J., Moher, D., 2009. The PRISMA statement for reporting systematic reviews and meta-analyses of studies that evaluate healthcare interventions: explanation and elaboration. BMJ 339, b2700. https://doi.org/10.1136/bmj.b2700.

Lyoo, C.H., Ikawa, M., Liow, J.-S., Zoghbi, S.S., Morse, C.L., Pike, V.W., Fujita, M., Innis, R.B., Kreisl, W.C., 2015. Cerebellum can serve As a pseudo-reference region in alzheimer disease to detect neuroinflammation measured with PET radioligand binding to translocator protein. J. Nucl. Med. 56, 701–706. https://doi.org/10.2967/jnumed.114.146027.

Meda, L., Cassatella, M.A., Szendrei, G.I., Otvos L Jr, Baron, P., Villalba, M., Ferrari, D., Rossi, F., 1995. Activation of microglial cells by β-amyloid protein and interferon-γ. Nature 374, 647–650. https://doi.org/10.1038/374647a0.

Morales, I., Jiménez, J.M., Mancilla, M., Maccioni, R.B., 2013. Tau oligomers and fibrils induce activation of microglial cells. J. Alzheimers Dis. 37, 849–856. https://doi.org/10.3233/JAD-131843.

Okello, A., Edison, P., Archer, H.A., Turkheimer, F.E., Kennedy, J., Bullock, R., Walker, Z., Kennedy, A., Fox, N., Rossor, M., Brooks, D.J., 2009. Microglial activation and amyloid deposition in mild cognitive impairment: a PET study. Neurology 72, 56–62. https://doi.org/10.1212/01.wnl.0000338622.27876.0d.

Parbo, P., Ismail, R., Hansen, K.V., Amidi, A., Mårup, F.H., Gottrup, H., Brændgaard, H., Eriksson, B.O., Eskildsen, S.F., Lund, T.E., Tietze, A., Edison, P., Pavese, N., Stokholm, M.G., Borghammer, P., Hinz, R., Aanerud, J., Brooks, D.J., 2017. Brain inflammation accompanies amyloid in the majority of mild cognitive impairment cases due to Alzheimer's disease. Brain 140, 2002–2011. https://doi.org/10.1093/brain/awx120.

Parbo, P., Ismail, R., Sommerauer, M., Stokholm, M.G., Hansen, A.K., Hansen, K.V., Amidi, A., Schaldemose, J.L., Gottrup, H., Brændgaard, H., Eskildsen, S.F., Borghammer, P., Hinz, R., Aanerud, J., Brooks, D.J., 2018. Does inflammation precede tau aggregation in early Alzheimer's disease? A PET study. Neurobiol. Dis. 117, 211–216. https://doi.org/10.1016/j.nbd.2018.06.004.

Passamonti, L., Rodríguez, P.V., Hong, Y.T., Allinson, K.S.J., Bevan-Jones, W.R., Williamson, D., Jones, P.S., Arnold, R., Borchert, R.J., Surendranathan, A., Mak, E., Su, L., Fryer, T.D., Aigbirhio, F.I., O'Brien, J.T., Rowe, J.B., 2018. [11C]PK11195 binding in Alzheimer disease and progressive supranuclear palsy. Neurology 90, e1989–e1996. https://doi.org/10.1212/WNL.0000000000005610.

Schuitemaker, A., Kropholler, M.A., Boellaard, R., van der Flier, W.M., Kloet, R.W., van der Doef, T.F., Knol, D.L., Windhorst, A.D., Luurtsema, G., Barkhof, F., Jonker, C., Lammertsma, A.A., Scheltens, P., van Berckel, B.N.M., 2013. Microglial activation in Alzheimer's disease: an (R)-[11C]PK11195 positron emission tomography study. Neurobiol. Aging 34, 128–136. https://doi.org/10.1016/j.neurobiolaging.2012.04.021.

Serrano-Pozo, A., Mielke, M.L., Gómez-Isla, T., Betensky, R.A., Growdon, J.H., Frosch, M.P., Hyman, B.T., 2011. Reactive glia not only associates with plaques but also parallels tangles in Alzheimer's disease. Am. J. Pathol. 179, 1373–1384. https://doi.org/10.1016/j.ajpath.2011.05.047.

Suridjan, I., Pollock, B.G., Verhoeff, N.P.L.G., Voineskos, A.N., Chow, T., Rusjan, P.M., Lobaugh, N.J., Houle, S., Mulsant, B.H., Mizrahi, R., 2015. In-vivo imaging of grey and white matter neuroinflammation in Alzheimer's disease: a positron emission tomography study with a novel radioligand, [18F]-FEPPA. Mol. Psychiatry 20, 1579–1587. https://doi.org/10.1038/mp.2015.1.

Thal, D.R., Rüb, U., Orantes, M., Braak, H., 2002. Phases of A beta-deposition in the human brain and its relevance for the development of AD. Neurology 58, 1791–1800.

Tomasi, G., Edison, P., Bertoldo, A., Roncaroli, F., Singh, P., Gerhard, A., Cobelli, C., Brooks, D.J., Turkheimer, F.E., 2008. Novel reference region model reveals increased microglial and reduced vascular binding of 11C-(R)-PK11195 in patients with Alzheimer's disease. J. Nucl. Med. 49, 1249–1256. https://doi.org/10.2967/jnumed.108.050583.

Varrone, A., Mattsson, P., Forsberg, A., Takano, A., Nag, S., Gulyás, B., Borg, J., Boellaard, R., Al-Tawil, N., Eriksdotter, M., Zimmermann, T., Schultze-Mosgau, M., Thiele, A., Hoffmann, A., Lammertsma, A.A., Halldin, C., 2013. In vivo imaging of the 18-kDa translocator protein (TSPO) with [18F]FEDAA1106 and PET does not show increased binding in Alzheimer's disease patients. Eur. J. Nucl. Med. Mol. Imaging 40, 921–931. https://doi.org/10.1007/s00259-013-2359-1.

Varrone, A., Oikonen, V., Forsberg, A., Joutsa, J., Takano, A., Solin, O., Haaparanta-Solin, M., Nag, S., Nakao, R., Al-Tawil, N., Wells, L.A., Rabiner, E.A., Valencia, R., Schultze-Mosgau, M., Thiele, A., Vollmer, S., Dyrks, T., Lehmann, L., Heinrich, T., Hoffmann, A., Nordberg, A., Halldin, C., Rinne, J.O., 2015. Positron emission tomography imaging of the 18-kDa translocator protein (TSPO) with [18F]FEMPA in Alzheimer's disease patients and control subjects. Eur. J. Nucl. Med. Mol. Imaging 42, 438–446. https://doi.org/10.1007/s00259-014-2955-8.

Viechtbauer, W., 2010. Conducting meta-analyses in r with the metafor package. J. Stat. Softw. 36. https://doi.org/10.18637/jss.v036.i03.

Wells, G., Shea, B., O'Connell, D., Peterson, J., Welch, V., Losos, M., Tugwell, P., 2000. The Newcastle - Scale for Assessing the Quality of Nonrandomised Studies in meta-analyses.pDf [WWW Document]. (accessed 9.17.18). http://www.medicine.mcgill.ca/rtamblyn/Readings/The%20Newcastle%20-%20Scale%20for%20assessing%20the%20quality%20of%20nonrandomised%20studies%20in%20meta-analyses.pdf.

Wiley, C.A., Lopresti, B.J., Venneti, S., Price, J., Klunk, W.E., DeKosky, S.T., Mathis, C.A., 2009. Carbon 11-labeled Pittsburgh Compound B and carbon 11-labeled (R)-PK11195 positron emission tomographic imaging in Alzheimer disease. Arch. Neurol. 66, 60–67. https://doi.org/10.1001/archneurol.2008.511.

Wilms, H., Claasen, J., Röhl, C., Sievers, J., Deuschl, G., Lucius, R., 2003. Involvement of benzodiazepine receptors in neuroinflammatory and neurodegenerative diseases: evidence from activated microglial cells in vitro. Neurobiol. Dis. 14, 417–424.

Yasuno, F., Ota, M., Kosaka, J., Ito, H., Higuchi, M., Doronbekov, T.K., Nozaki, S., Fujimura, Y., Koeda, M., Asada, T., Suhara, T., 2008. Increased binding of peripheral benzodiazepine receptor in Alzheimer's disease measured by positron emission tomography with [11C]DAA1106. Biol. Psychiatry 64, 835–841. https://doi.org/10.1016/j.biopsych.2008.04.021.

Yasuno, F., Kosaka, J., Ota, M., Higuchi, M., Ito, H., Fujimura, Y., Nozaki, S., Takahashi, S., Mizukami, K., Asada, T., Suhara, T., 2012. Increased binding of peripheral benzodiazepine receptor in mild cognitive impairment-dementia converters measured by positron emission tomography with [^{11}C]DAA1106. Psychiatry Res. 203, 67–74. https://doi.org/10.1016/j.pscychresns.2011.08.013.

Yokokura, M., Mori, N., Yagi, S., Yoshikawa, E., Kikuchi, M., Yoshihara, Y., Wakuda, T., Sugihara, G., Takebayashi, K., Suda, S., Iwata, Y., Ueki, T., Tsuchiya, K.J., Suzuki, K., Nakamura, K., Ouchi, Y., 2011. In vivo changes in microglial activation and amyloid deposits in brain regions with hypometabolism in Alzheimer's disease. Eur. J. Nucl. Med. Mol. Imaging 38, 343–351. https://doi.org/10.1007/s00259-010-1612-0.

Yokokura, M., Terada, T., Bunai, T., Nakaizumi, K., Takebayashi, K., Iwata, Y., Yoshikawa, E., Futatsubashi, M., Suzuki, K., Mori, N., Ouchi, Y., 2017. Depiction of microglial activation in aging and dementia: positron emission tomography with [11C]DPA713 versus [11C](R)PK11195. J. Cereb. Blood Flow Metab. 37, 877–889. https://doi.org/10.1177/0271678X16646788.